Cement and Concrete Research 40 (2010) 531–536

Contents lists available at ScienceDirect

Cement and Concrete Research

journal homepage: http://ees.elsevier.com/CEMCON/default.asp

ASR expansion behavior of recycled glass fine aggregates in concrete

Andrea Saccani *, Maria Chiara Bignozzi

Dipartimento di Chimica Applicata e Scienza dei Materiali, University of Bologna, Via Terracini 28, Bologna, Italy

ARTICLE INFO

Article history:
Received 31 October 2008
Accepted 3 September 2009

Keywords:
Alkali-Silica-Reaction (C)
Expansion (C)
Recycled Industry Cullets (E)
Glass composition (B)
Aggregate replacement (D)

ABSTRACT

The alkali–silica-reaction (ASR) expanding behavior of different types of glass, all derived from cullet with different chemical composition, has been investigated. The glass reactivity was determined in different alkaline solutions based on sodium and/or calcium hydroxide to simulate concrete environment. The expansion of mortar containing different amounts of the investigated glass as fine aggregate has been carried out in different conditions: data collected underline a different response of glass towards the alkaline environment. Soda–lime glass shows negligible expansion, lead–silicate glass always generates expanding trends while boro–silicate glass has different behaviors depending on its colour. An attempt to link the behavior to the solubility and chemical reactivity of the glass is proposed.

1. Introduction

Alkali–silica-reaction (ASR) is definitely one of the most deleterious events that can occur in concrete: the reaction products are expansive and lead to crack formation with disruptive effects. For this reason, high quality aggregates need to be used in building engineering as prescribed by the European standards EN 12620 “Aggregates for concrete” [1], and EN 13139 “Aggregates for mortar” [2], which define the characteristics and limits to obtain CE certification. This official mark is particularly important if the use of recycled and unconventional aggregates is considered. In fact, the exploitation of unconventional aggregates has been recently encouraged by specific laws all over Europe and has brought environmental advantages, such as safeguarding of not renewable raw materials and decrease of landfill disposal.

Recycled glass has already been used as concrete aggregate [3–7], however, its amorphous nature can promote and develop ASR. As recycled glass may come from many sources, for example separated municipal waste, industrial waste, TV cathode-ray tubes (CRT), etc., it is very important to investigate if and how glass composition influences ASR.

In this work, different types of glass (soda–lime, boro–silicate, lead–silicate glass), whose origin will be specified in details further on, have been studied to test their reactivity towards alkalis: all glass types have been used as aggregates replacing up to 35 wt.% of sand. Cullet used in this research came from food, pharmaceutical and house-ware glass. These amorphous materials, on account of their contact with food or drugs, must fulfil safety requirements concerning hazardous elements leachability, according to European Directive 94/62/EC [8], (and following issues) on packaging and packaging waste. Moreover, European Directive 91/156/CEE [9] on waste (and following modifications) moves each European country towards recycling cullet (e.g. in new glass production, in manufacturing cement matrix conglomerates, etc.). Some glass types do contain heavy metals which could be progressively leached due to the high alkalinity of cementitious materials; however, previous studies [10,11] have demonstrated that suitable formulations of cement composites can efficiently restrain this process.

This study investigates the relation between glass composition and its potentially deleterious behavior in concrete by expansion testing under different experimental conditions. Moreover, through SEM-EDS analysis, an assessment of the materials is carried out.

2. Experimental details

2.1. Materials

Cement: Type I Portland cement 52.5 R with an equivalent alkali content (Na_2Oeq) of 0.65 wt.% has been used.

Aggregates: quartz sand with normalized grain size distribution according to EN 196-1 [12] has been used.

Glass: soda–lime glass (hereafter referred as SL) coming from beverage containers cullet (kindly supplied by Bormioli Rocco, Fidenza (PR) Italy), uncoloured boro–silicate glass (BS-U) and amber boro–silicate glass (BS-A) coming from pharmaceutical containers cullet (kindly supplied by Bormioli Rocco, Fidenza (PR) Italy), lead–silicate glass (CR), coming from production of tableware, giftware and home décor items in crystal (kindly supplied by CALP, Colle di Val d'Elsa, Siena Italy). The chemical composition (wt.%) of the investigated materials, as determined by inductively coupled plasma-optical emission spectrometry (ICP-OES Perkin Elmer, Optima 3200

* Corresponding author. Fax: +0039 0512090322.
E-mail address: andrea.saccani@unibo.it (A. Saccani).

0008-8846/$ – see front matter © 2009 Elsevier Ltd. All rights reserved.
doi:10.1016/j.cemconres.2009.09.003

XL), is reported in Table 1: values below 50×LLD (lower limit of detection), being unreliable for modelling have been inserted in *italics*. Virgin sample material was prepared for bulk chemical analysis by pulverization to <125 µm and drying at 105 °C. Next, 200 mg of the pre-dried powder was digested in excess HNO_3 and HF, and evaporated until dry. This residue was then redissolved in 1 N HNO_3 and diluted to appropriate volume with double distilled water. Separate 100 mg amounts were microwave-digested in excess acid (5 N HNO_3) for 20 min at 200 °C.

The investigated glass samples were dry comminuted in a laboratory steel jaw crusher to get particles between 0.075 and 2.00 mm, with size distribution close to that of normalized sand (EN 196-1), (Fig. 1). Chemical analysis of the sand-like glass did not provide significant variation from those of Table 1.

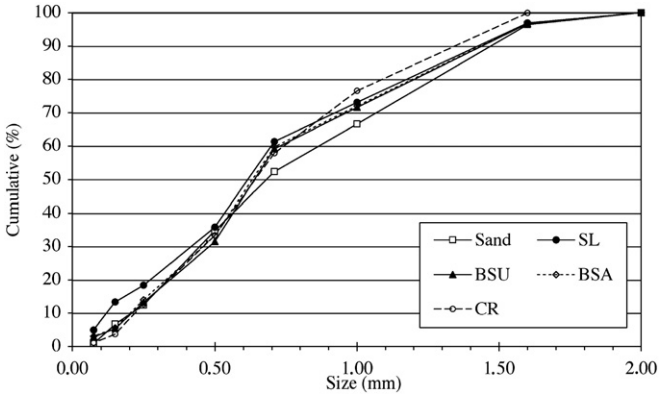

Fig. 1. Grain size distribution of crashed glass and normalized sand.

2.2. Mortar and curing

Mortar samples were prepared by a Hobarth planetary mixer with 1/3 binder/aggregate and 1/2 water/binder ratios, following the procedure described in EN 196-1. Glass replaces aggregates at 10, 25 and 35 wt. %; reference samples without glass were also prepared for comparison sake. Mortar workability (measured by flow table test according to EN 1015-3 [13]) decreased as the amount of replaced sand increased, but at the same content of replacement the different samples have comparable workability (mortar without glass, mean diameter: 17 cm; mortar with 10 wt.% glass replacing sand, mean diameter: 15–16 cm; mortar with 25 wt.% glass replacing sand, mean diameter: 12–14 cm; mortar with 30 wt.% glass replacing sand, mean diameter 11–12 cm).

40×40×160 mm prisms were cast to investigate mortar dimensional stability. Mortar samples were cured for 1 day at 25 °C and 100% R.H. then submitted to accelerated curing at 80 °C in a 1 N NaOH solution. This procedure closely resembles ASTM C1260 standard [14]. In order to investigate the effect of temperature and alkali concentration, mortar prisms with 25 wt.% glass replacing sand were prepared by adding NaOH directly to the mixing water, thus providing an overall Na_2Oeq content of 2.5 wt.%. These samples have been cured at 25 and 38 °C at 100% R.H. for 240 days. The expansion tests for all specimens were carried out simultaneously in three different curing chambers operating at 25, 38 and 80 °C respectively.

2.3. Tests and characterizations

2.3.1. Expansion tests

Mortar stability was determined by means of a mechanical comparator (0.001 mm accuracy) on samples cooled at room temperature: the detailed procedures are elsewhere reported [15] and are close to that as prescribed by ASTM C1260 (80 °C) and ASTM C227 (38 °C) [16].

Table 1
Glass composition determined by ICP-OES.

Oxide	Investigated glass				
	LLD	BS-U	BS-A	SL	CR
SiO_2	0.07	68.1	65.3	70.2	61.7
Al_2O_3	0.04	5.64	5.88	2.06	*0.04*
B_2O_3	0.001	11.6	10.7	0.69	0.72
MgO	0.0007	*0.003*	*0.004*	1.47	*0.03*
CaO	0.002	1.53	1.42	11.1	*0.01*
Na_2O	0.04	8.06	8.02	13.1	3.96
K_2O	0.024	1.24	1.16	1.21	6.96
ZnO	0.006	0.82	0.78	*0.01*	0.90
BaO	0.001	2.95	2.86	0.12	*0.005*
Fe_2O_3	0.014	*0.02*	0.78	*0.02*	*0.03*
TiO_2	0.0003	*	2.89	0.01	*
PbO	0.0043	*	*	*	25.3
Sb_2O_3	0.007	*	*	*	*0.26*
Sum		99.9	99.8	100.0	99.5

*Not detected.
Data in *italics* have values below 50×LLD.

2.3.2. Solubility

Glass samples in the shape of disks (diameter: 10±1.0 mm; thickness: 3.0±0.1 mm), free from porosities were obtained by direct casting from the melt (operating temperature: 1400 °C). Glass disks were stored in a static mode in three different alkaline solutions at 80 °C with a solid surface area/solution volume ratio (S/V) of 2.3 cm^{-1}. The tested solutions were the following: 1 N NaOH, saturated lime water and 1 N NaOH solution saturated with $Ca(OH)_2$. The last of the three is the one which best reproduces the mortar environment on account of the contemporary presence of sodium and calcium ions. Glass weight change and pH solutions were recorded for 30 days. The pH was always above 12.5 (for saturated lime water) and 13.4 (for 1 N NaOH and 1 N NaOH solution saturated with $Ca(OH)_2$) without significant variations during the tests.

2.3.3. Scanning electron microscopy (SEM) and energy dispersive X-ray spectroscopy (EDS)

Morphological investigations were carried out by SEM (Philips XL 20 equipped by secondary electrons detector) on samples of mortar fractured surfaces after expansion and glass, following solubility tests. Each sample was coated by gold (morphological examination) or carbon (morphological characterization plus EDS analysis). Polished thin sections (about 50 µm thick) were also prepared by dry cutting with a diamond saw the 40×40×160 mm mortar samples, which were treated with carborundum paper. Small particles were removed by air-blowing, samples were then treated with acetone to eliminate water and sputtered with carbon: the resulting samples were analysed with EDS detector (Genesis 2000, Philips). Operating conditions were set at 10 kV with a probe current of 9±2 nA; the vacuum condition was below 10^{-4}Torr: a typical analysis lasted for about 300 s with approximately 25% dead time. At this stage of the experimental work, boron could not be evaluated due to the hardware configuration of the detector. The LLD of the technique are about 0.1 wt.% for elements with atomic weight higher than Mg and 0.3 wt.% for lighter elements. The EDS analysis was performed without internal standard: as a consequence the reported values (expressed as oxides normalized to 100) should be considered only as indicative of the phases composition and affected by the intrinsic uncertainty related to the undefined volumes of X-ray emission.

3. Results

3.1. Expansion tests

Fig. 2 shows the expansion of mortar after 14 days in 1 N solution of NaOH at 80 °C as a function of the glass content replacing sand.

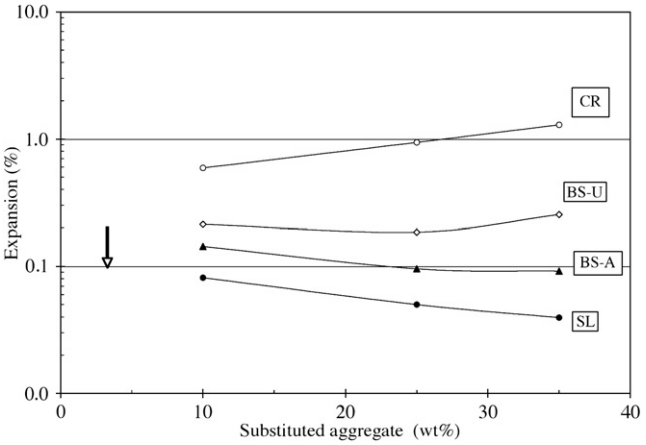

Fig. 2. Mortars' expansion at 14 days as a function of substituted sand (conditions: 80 °C in 1 N NaOH solution).

While the expansion of mortar containing SL and BS-A glass hardly ever exceeds the limit of 0.1% l/l (only when BS-A replaces 10 wt.% of sand, the relevant mortar expansion is slightly above this limit set by ASTM C1260), BS-U and CR modified mortar undergo expansion well above the previous limit. Data collected at 38 and 25 °C at 100% R.H. (Figs. 3 and 4), although showing lower expansion values, confirm the experimental trend previously observed. Indeed, temperature and alkalis' content available for ASR affect the extent of expansion, but not the relative reactivity of the glass.

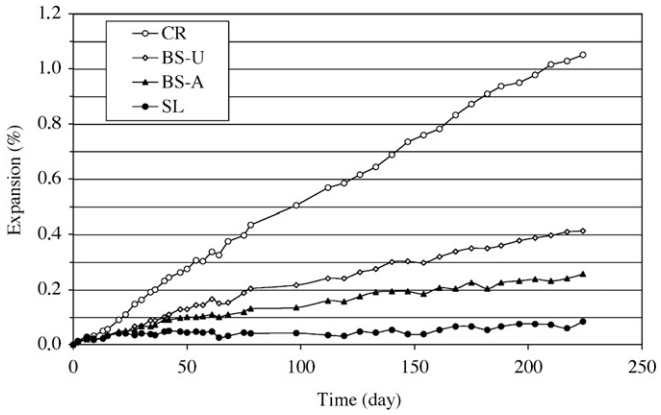

Fig. 3. Mortars' expansion vs time at 38 °C and R.H. 100%.

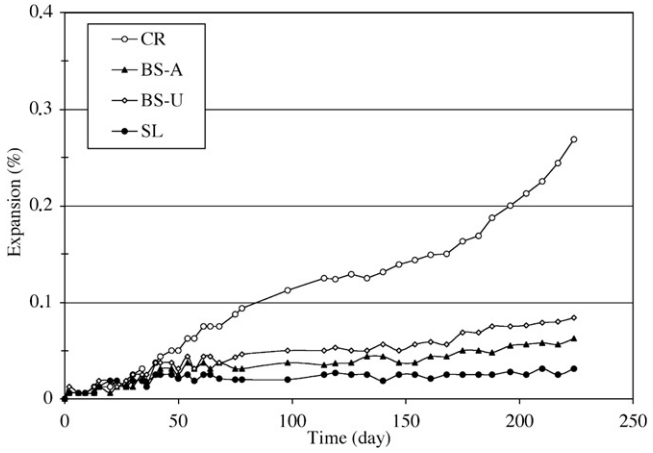

Fig. 4. Mortars' expansion vs time at 25 °C and R.H. 100%.

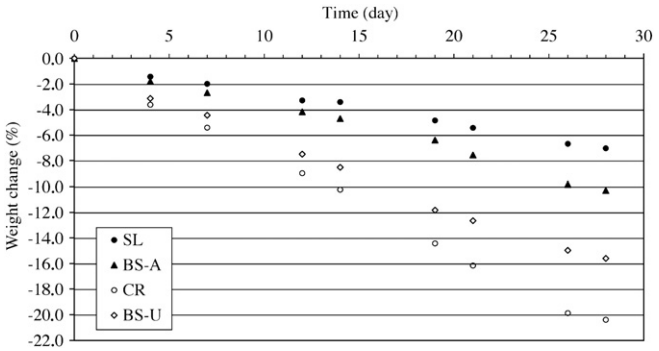

Fig. 5. Solubility of glass vs time in 1 N NaOH solution.

3.2. Glass solubility

Figs. 5–7 report the glass solubility (determined as a weight change %) versus time in 1 N NaOH, saturated lime water and 1 N NaOH solution saturated with $Ca(OH)_2$, respectively.

1 N NaOH solution is the most severe as to what concerns the rate of dissolution: CR glass shows the highest dissolution rate, SL is the most stable and BS-A is less soluble than BS-U. Experimental data determined in saturated lime water show that the presence of Ca^{2+} ions in the environment, hinders the dissolution of glass, irrespective of chemical composition. In 1 N NaOH solution saturated with $Ca(OH)_2$, after an initial induction period at almost constant weight, the trend of solubility is similar to that in 1 N NaOH solution. SEM observations of the glass surfaces of SL, BS-U and BS-A show that the dissolution in 1 N NaOH solution and 1 N NaOH solution saturated with $Ca(OH)_2$ proceeds on the whole surface, through the creation and subsequent detachment of thin layers of material (Figs. 8 and 9). EDS semi-quantitative analysis underlines that the detaching layers

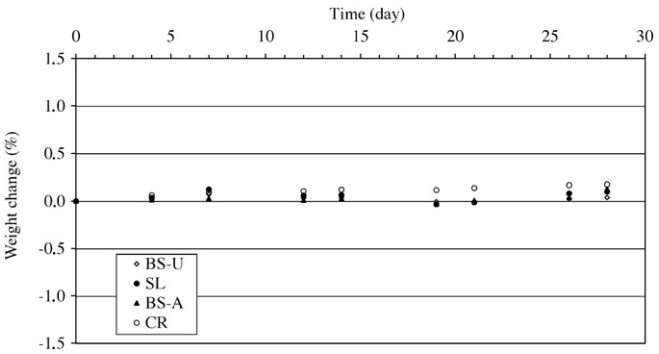

Fig. 6. Solubility of glass vs time in saturated lime water.

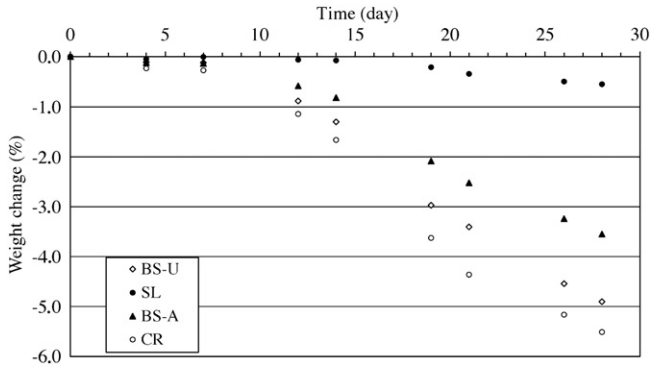

Fig. 7. Solubility of glass vs time in 1 N NaOH solution saturated with $Ca(OH)_2$.

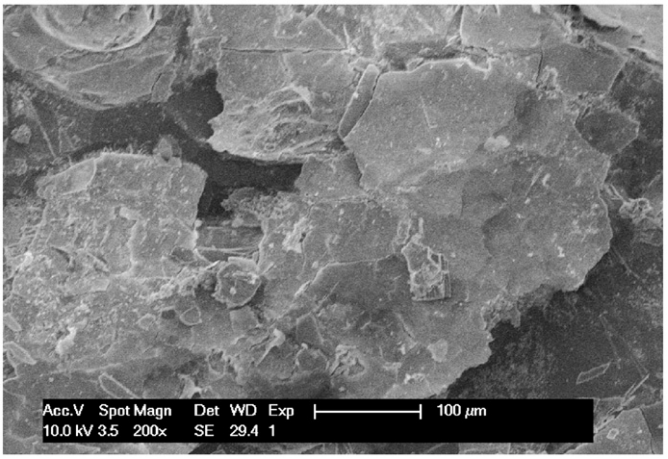

Fig. 8. Glass surface of BS-A in 1 N NaOH solution saturated with $Ca(OH)_2$ at 14 days and 80 °C.

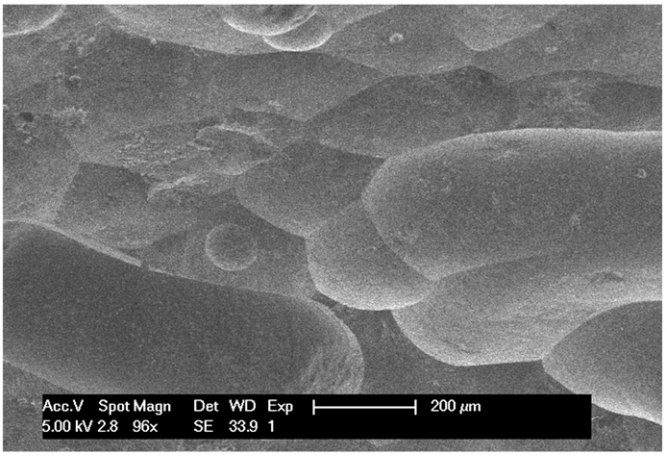

Fig. 10. Surface of sample CR in 1 N NaOH solution saturated with $Ca(OH)_2$ at 14 days and 80 °C.

have lower concentration of silica than the bulk material in 1 N NaOH solution and 1 N NaOH solution saturated with $Ca(OH)_2$, higher concentration of sodium oxide and sodium, calcium and aluminium oxides in the two conditions, respectively. Moreover, BS-U detaching layers are richer in titanium and BS-A ones are richer in both titanium and iron than the relevant bulk materials. As to CR, a rather homogeneous surface was observed, with composition close to that of the original glass (Fig. 10): very small areas, covered by filament-like formations, mainly constituted by sodium and silicon oxides were observed (Fig. 11).

3.3. ASR gel composition

Although at a different quantitative level, ASR gels were present in all mortar samples, with morphologies close to those found in natural reactive aggregates. As an example, Fig. 12 reports the microstructure of the fracture surface of a mortar containing 25 wt.% CR replacing sand and cured at 80 °C after 14 days. Table 2 reports the semi-quantitative oxide composition of the gels in 25 wt.% glass replacing sand mortar, cured at 80 °C. The examined gels are those formed next to the glass aggregate surface. Chemical composition was determined by EDS on carbon sputtered thin specimens without the use of internal standards: the reported values are the average of at least 10 different analyses. SL gel exhibits a composition consistent with those found in literature [17], while BS-U and BS-A gels contain elements like Fe, Ba and Ti and CR gel contains Pb.

4. Discussion

Although sharing common chemical/physical characteristics (disordered structure, absence of porosity, high amount of silica), glass specimens of different composition exhibit a quite different response to ASR. CR provokes, in accelerated conditions, a deleterious effect (expansion above 0.2% l/l) even at low content (10 wt.%): expansion steadily increases as the amount of substituted sand increases, and the previous limit is exceeded also at room temperature. On the other end, SL remains under safety limits up to a 35 wt.% substitution. Small compositional differences are sufficient to turn the behavior of boro–silicate glass from innocuous to deleterious (BS-A *vs* BS-U). Concerning the possibility of recycling these waste typologies, the first conclusion that can be drawn is that a systematic study on different types of glass should be carried out in order to identify the expanding compositions. Moreover, well defined quality and process control should be set and applied in the treatment of post-consumer glass in order to avoid unexpected and undesired concrete failure. From the scientific point of view, the attention is instead focussed on explaining the origin of such a different behavior. Expansion is not directly linked to the silica content in the glass used as aggregate (Table 1): indeed, SL has the highest SiO_2 content but shows the lowest expansion. Other parameters must be thus responsible for reactivity: solubility tests highlight a direct correlation between the amount of the dissolved glass (i.e. the amount of silica that will be available in solution for ASR gel formation) and the extent of mortar

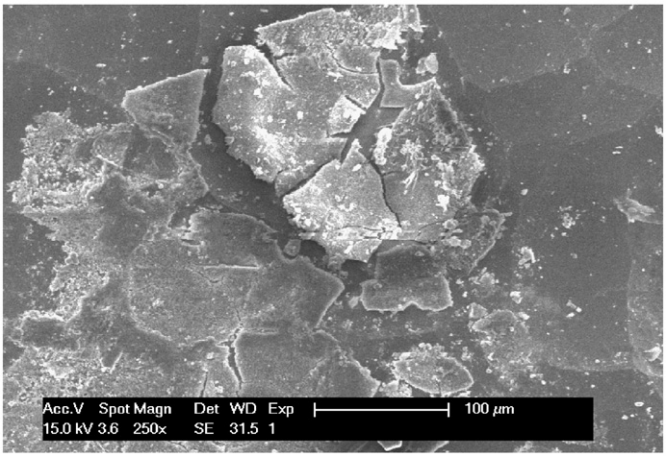

Fig. 9. Glass surface of BS-U in 1 N NaOH solution saturated with $Ca(OH)_2$ at 14 days and 80 °C.

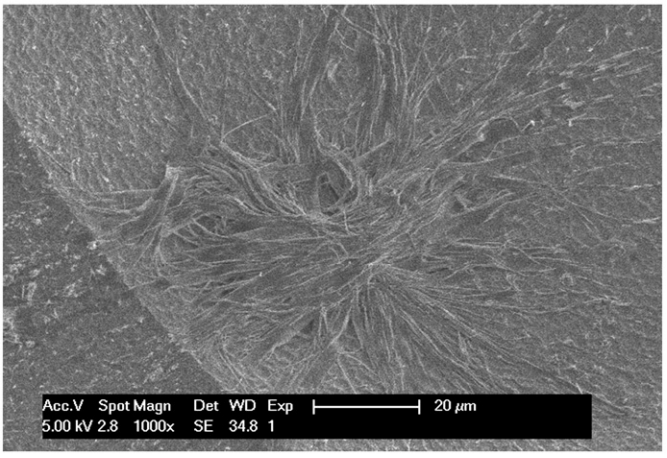

Fig. 11. Small formations on CR sample in 1 N NaOH solution saturated with $Ca(OH)_2$ at 14 days.

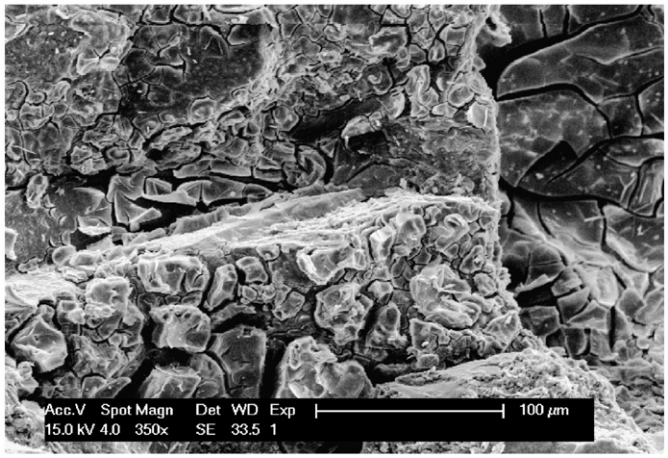

Fig. 12. Fracture surface of a 25% substituted CR mortar at 14 days in NaOH at 80 °C.

expansion. Different mechanisms seem to control the solubility of the investigated glass samples. In the case of CR, a homogeneous dissolution process affects the main phase of the crystal glass leading to the network dissolution; a secondary phase (observed by SEM) is present in the glass, but its volume and dimension seem not significantly influence the dissolution process. As to what concerns SL, BS-A and BS-U, ion-exchange and selective leaching seem to be the main processes leading to the formation of a surface layer with a different chemical composition from the bulk, which precedes the dissolution step [18]. These processes, where ion' diffusion plays a fundamental role, are particularly important for these types of aggregates, completely free from porosities. The presence of small amounts of Fe, Ti and Ba creates a barrier that efficiently hinders glass solubility, thus explaining the different behavior of BS-U versus BS-A. The stabilizing effect of iron, titanium and barium towards solubility in boro–silicate glass, as well as the high solubility of lead–silicate glass are consistent with available literature data [19,20]. It is also important to underline the buffering effect of Ca^{2+} ions (Figs. 6 and 7) as to what concerns solubility: indeed the increase in Ca^{2+} concentration decreases glass dissolution [21]. The presence of lead and/or barium cations in solution can decrease the concentration of calcium ones, on account of the higher or comparable solubility of their hydroxides; this effect can thus produce, in concrete, a further increase in glass dissolution and could explain the high reactivity of CR glass as well as that of cathode-ray tubes (CRT) glass elsewhere observed [22]. Our experimental work thus confirms that glass with different chemical composition releases, *ceteris paribus*, different amounts of SiO_2.

The formation of ASR gel from the dissolved silica is the last step of the overall process: according to some theories [23] (which are however still disputed [24]), the presence of a high amount of calcium ions creates gels with lower swelling capacity. This is confirmed by SL gel as it results from EDS analysis, which underlines the presence of a high amount of calcium. As to what concerns boro–silicate glass, according to the electrical double layer theory [25] a positive effect on reducing the swelling capacity of the gel may be exerted by the presence of small and highly charged Fe^{3+} or Ti^{4+} cations [26]. For CR the situation is more complex: EDS underlines the presence of Pb^{2+} and Ca^{2+} in the investigated gel. It can be assumed that Pb^{2+} cations (having lower charge density than Ca^{2+} ones) are present in the gel with a negative effect on its swelling capacity or that Pb^{2+} ions, having greater dimension than calcium ones (0.126 vs 0.108 nm), may hardly diffuse into the gel. Indeed, the size of the ion is one of the most important factors that governs the mobility in minerals [27]. According to this, Pb could be present as a second separated phase (such as hydroxide) closely mixed with the ASR gel: this hypothesis can be supported by the higher dispersion of data in the determined CR gel composition. However, EDS does not allow to exactly determine the structure of the gel, hence ^{29}Si-NMR studies are requested according to literature data [17,28,29] to confirm this hypothesis. The already mentioned competition of Pb^{2+} ions (but also of Ba^{2+}) with Ca^{2+} ones in solution, could consequently induce a decrease of calcium concentration in the gel, generating more expanding conditions.

Table 2
Average ASR oxide gel composition normalized to 100 from EDS (LLD: 0.3% for elements with atomic number < Mg, 0.1% for elements with atomic number > Mg).

Oxide	CR	±Δ	SL	±Δ	BS-U	±Δ	BS-A	±Δ
SiO2	45.8	6.8	54.9	3.1	59.0	2.7	58.4	3.3
Al_2O_3	0.4	0.2	2.0	0.4	8.1	1.5	8.9	1.9
CaO	22.0	5.7	35.7	2.9	5.3	0.9	4.3	0.9
MgO	0.4	0.2	*	*	*	*	*	*
Na_2O	14.8	4.6	4.2	0.8	22.4	1.2	21.2	*
K_2O	3.7	1.2	3.3	0.2	4.0	0.8	2.1	*
PbO	12.9	8.4	*	*	*	*	*	*
TiO_2	*	*	*	*	*	*	3.4	1.1
Fe_2O_3	*	*	*	*	*	*	0.6	0.3
BaO	*	*	*	*	1.2	0.2	1.0	0.2

*Not detected; Δ = standard deviation.

5. Conclusions

The main conclusions from the experimental work carried out can be as follows:

- glass chemical composition strongly influences the expansion behavior of mortar samples containing cullet as aggregate. In view of glass recycle broadening, expanding compositions should be determined and selective procedures introduced for the treatment of post-consumer glass;
- the investigated experimental conditions highlight that CR glass always leads to critical expanding conditions for the relevant mortar samples;
- a direct correlation between glass solubility and mortar expansion has been underlined and a buffering effect of Ca^{2+} towards glass solubility has been confirmed. The solubility process involves a homogeneous network dissolution in CR glass, whereas detaching layers are formed in all the other glass types. The solubility of boro–silicate glass is strongly influenced by the presence of Fe, Ba and Ti oxides;
- ASR gel compositions, as determined by EDS, depend on chemical composition of the original glass used as aggregate. The electrical charge and dimension of the ions in the gel are important parameters in determining its characteristics, such as the swelling capacity.

References

[1] European standard EN 12620 Aggregates for concrete, CEN, Brussels, 2002.
[2] European standard EN 13139 Aggregates for mortar, CEN, Brussels, 2002.
[3] M.C. Bignozzi, F. Sandrolini, Wastes by glass separated collection: a feasible use in cement mortar and concrete, in: M.C. Limbachiya, J.J. Roberts (Eds.), Proceedings of the International Conference Sustainable waste management and recycling Kingston University, London, Thomas Telford, London, UK, September 17–24 2006.
[4] V. Corinaldesi, G. Gnappi, G. Moriconi, A. Montenero, Reuse of ground waste glass as aggregate for mortar, Waste Manage. 25 (2) (2005) 197–201.
[5] A. Shayan, A. Xu, Value added utilisation of waste glass in concrete, Cem. Concr. Res. 34 (2004) 81–89.
[6] Y. Shao, T. Lefort, S. Moras, D. Rodriguez, Studies on concrete containing ground waste glass, Cem. Concr. Res. 30 (2000) 91–100.
[7] W. Jin, C. Meyer, S. Baxter, Glas–crete: concrete with glass aggregate, ACI Mater. J. 97 (2000) 208–213.
[8] European Parliament and Council Directive 94/62/EC of 20 December 1994 on packaging and packaging waste, Off. J. L 365 (31/12/1994) 10–23.
[9] Council Directive 91/156/EEC of 18 March 1991 amending Directive 75/442/EEC on waste, Off. J. L 078 (26/03/1991) 32–37.

[10] Q.Y. Chen, M. Tyrer, C.D. Hills, X.M. Yang, P. Carey, Immobilisation of heavy metal in cement based solidification/stabilisation: a review, Waste Manage. 29 (2009) 390–403.
[11] G. Bar-Nes, A. Katz, Y. Peled, Y. Zeiri, The mechanism of cesium immobilization in densified silica fume blended cement pastes, Cem. Concr. Res. 38 (2008) 667–674.
[12] European Standard EN 1015-3 Methods of Test for Mortar for Masonry — Part 3: Determination of Consistence of Fresh Mortar (by flow table), CEN, Brussels, 2007.
[13] European Standard EN 196-1 Methods of Testing Cement — Part 1: Determination of Strength, CEN, Brussels, 2005.
[14] American Standard ASTM C1260 Standard test method for potential alkali reactivity of aggregates, American Society for Testing and Materials, West Conshoshockner/PA, 2007.
[15] A. Saccani, V. Bonora, P. Monari, Laboratory short-term ASR: a contribution, Cem. Concr. Res. 31 (2001) 739–742.
[16] American Standard ASTM C227 Standard test method for potential alkali reactivity of cement aggregate combination, American Society for Testing and Materials, West Conshoshockner/PA, 2003.
[17] X. Hou, R.J. Kirkpatric, L.J. Struble, P.J.M. Monteiro, Structural investigation of ASR, J. Am. Ceram. Soc. 88 (4) (2005) 943–949.
[18] D.E. Clark, E.L. Yen-Bower, Corrosion of glass surfaces, Surf. Sci. 100 (1980) 53–70.
[19] P. Trocellier, S. Djanathany, J. Chene, A. Haddi, A.M. Brass, S. Poissoneet, F. Farges, Chemical durability of alkali–borosilicate glass studied by analytical SEM, IBA, isotopic-tracing and SIMS, Nucl. Instrum. Methods Phys. Res. B 240 (2005) 337–344.
[20] N. Carmona, M. Garcia-Heras, C. Gil, M.A. Villegas, Chemical degradation of glasses under simulated marine medium, Mater. Chem. Phys. 94 (2005) 92–102.
[21] S. Chatterji, Chemistry of the alkali–silica reaction and testing of aggregates, Cem. Concr. Compos. 27 (2005) 788–795.
[22] C. Morrison, Reuse of CRT glass as aggregate in concrete, International Conference on Sustainable Waste Management and Recycling: Glass Waste, Kingston University, Thomas Telford Services Ltd, September 14–15, 2005.
[23] P.J.M. Monteiro, K.S. Wang, G.M.C. dos Santos, W.P. de Andreade, Influence of mineral admixture on the ASR reaction, Cem. Concr. Res. 27 (1997) 1899–1909 and references therein.
[24] X. Hou, L.J. Struble, R.J. Kirkpatrick, Formation of ASR gels and the roles of CSH and portlandite, Cem. Concr. Res. 34 (2004) 1683–1696 and references therein.
[25] M. Prezzi, P.J.M. Monteiro, G. Sposito, ASR part 2: the effect of chemical admixtures, ACI Mat. J. 95M1 (1998) 3–10.
[26] E.J.W. Whitteker, R. Muntus, Ionic radii for use in geochemistry, Geochim. Cosmochim. Acta 34 (1980) 945–956.
[27] E. Dowty, Crystal chemical factors affecting the mobility of ions in minerals, Am. Mineral. 65 (1980) 174–182.
[28] X.D. Cong, R.J. Kirkpatric, S. Diamond, Silicon-29 Mas NMR spectroscopic investigation of ASR product gels, Cem. Concr. Res. 23 (1993) 811–823.
[29] L.D. Mitchell, J.J. Beadoin, P. Grattan-Bellew, The effects of lithium hydroxide solution on alkali silica reaction gel created with opal, Cem. Concr. Res. 34 (2004) 641–649.